

LOCAL AND GLOBAL SIMILARITY IN TURBULENT TRANSFER OF HEAT, WATER VAPOUR, AND CO₂ IN THE DYNAMIC CONVECTIVE SUBLAYER OVER A SUBURBAN AREA

RYO MORIWAKI* and MANABU KANDA

Department of Civil Engineering, Tokyo Institute of Technology, 2-12-1 O-okayama, Meguro-ku, Tokyo 152-8552, Japan

(Received in final form 20 September 2005 / Published online: 30 December 2005)

Abstract. We investigated the ‘local’ and ‘global’ similarity of vertical turbulent transfer of heat, water vapour, and CO₂ within an urban surface layer. The results were derived from field measurements in a residential area of Tokyo, Japan during midday on fair-weather days in July 2001. In this study, correlation coefficients and quadrant analysis were used for the evaluation of ‘global’ similarity and wavelet analysis was employed for investigating ‘local’ similarity. The correlation coefficients indicated that the transfer efficiencies of water vapour and CO₂ were generally smaller than that of heat. Using wavelet analysis, we found that heat is always efficiently transferred by thermal and organized motions. In contrast, water vapour and CO₂, which are passive quantities, were not transferred as efficiently as heat. The quadrant analyses showed that the heat transfer by ejection exceeded that by sweep, and the ratios of ejection to sweep for water vapour and CO₂ transfer were less than that for heat. This indicated that heat is more efficiently transferred by upward motions and supported the findings from wavelet analysis. The differences of turbulent transfer between heat and both CO₂ and water vapour were probably caused both by the active role of temperature and the heterogeneity in the source distribution of scalars.

Keywords: Correlation coefficient, Flux-variance relationship, Tower measurement, Turbulent transfer of scalars, Urban surface layer, Wavelet analysis.

1. Introduction

The use of Monin–Obukov similarity theory, hereafter MOS theory, to predict surface fluxes from associated variances, known as the flux-variance method, is a practical method to estimate the turbulent fluxes of momentum, heat, and water vapour. This method has been well developed for smooth, homogeneous surfaces such as grass, crop, and forest (e.g., Tillman, 1972; Weaver, 1990). Ohtaki (1985) found that the method has also been used to determine the turbulent statistics of carbon dioxide

* E-mail: moriwaki@ide.titech.ac.jp

(CO₂) concentration over a homogeneous crop. However, in recent years, studies have noted that the latent heat flux comparisons between flux-variance predictions and eddy-correlation measurements are inferior to those of sensible heat for the same site (e.g., Asanuma and Brutsaert, 1999; Katul and Hsieh, 1999). Katul et al. (1995) demonstrated that the non-uniformity in water vapour sources reduced the flux-variance-predicted latent heat flux when compared to the eddy-correlation-measured flux. Although many researchers have discussed the similarity between temperature and humidity transfer (e.g., Wesely, 1988; Mahrt, 1991 and 2000; De Bruin et al., 1993 and 1999; Katul et al., 1995 and 1997a; Andreas et al., 1998; Sempreviva and Høstrup, 1998), little attention has been devoted to CO₂ transport.

The urban field experiment of Roth and Oke (1995) indicated that the empirical flux-variance relationship is not applicable for water vapour transfer due to the heterogeneity of water vapour sources. However, knowledge on the flux-variance relationships in the urban surface layer is still much less than that in low-roughness homogeneous surfaces. In addition, the monitoring of CO₂ flux in urban areas has become an important issue in urban surface studies (e.g., Grimmond et al., 2002; Moriwaki and Kanda, 2004). In urban environments there exists the difference in ground sources and sinks of heat, water vapour, and CO₂; e.g., Moriwaki and Kanda (2004) showed that the main source of H₂O is from vegetation and that of CO₂ is from houses, transportation, and human exhalations in a suburban area in Tokyo, Japan. Therefore, further inquiries on the features of turbulent transfer of scalars are needed not only for heat and water vapour, but also for CO₂.

In this study, we analyzed data on the turbulent transfer of heat, water vapour, and CO₂ over the suburban surface. We examined the 'global' similarity of the vertical transfer of scalars that had different source distributions and different physical behaviour by using the turbulent linear correlation coefficients, a method previously used by Roth and Oke (1995). Also, we used wavelet analysis to determine the time-scale characteristics of the turbulent transfer of scalars for the evaluation of the 'local' similarity. Finally, quadrant analysis was used to determine the contributions of sweep or ejection motion to the total fluxes.

2. Method

2.1. FIELD EXPERIMENT

The experiment was done during July 2001 in a low-storied residential area in Kugahara, Tokyo, Japan (35°34' N, 139°41' E). A 29-m tower (without guy lines) was installed in the backyard of a home. The residential area



Figure 1. View to the west from the 20 m height of the tower.

consists of houses with a mean height of 7.3 m, paved roads, and small playgrounds. A view from the tower is shown in Figure 1. Flat, uniform terrain extended over 1 km to the south, west, and north from the tower. The terrain within 200 m to the east is gently slanting down with an inclination angle of 5.7° . Within a circle of 500 m radius centred on the site, about 33% of the area was buildings, 22% was vegetation, and 23% was impervious space such as paved roads and concrete (Table I). A general description of the climatology and energy exchanges between the surface and the atmosphere at this site is described in Moriwaki and Kanda (2004). Using data from the same tower, they showed that the net CO₂ flux was always upward throughout the year with an annual flux that was six times larger than the downward CO₂ flux at a temperate deciduous forest in Oak Ridge in the U.S.A. (Baldocchi and Wilson, 2001).

A sonic anemometer (USA1, Metek GmbH) and an infrared CO₂/H₂O open-path analyzer (LI-7500, LI-COR) were installed at the tower top (29 m), which is about 4 times the canopy height. To avoid any influences of flow distortion by the tower, the instruments were located at a distance of 1.5 times the lateral width away from the tower (Kaimal and Finnigan, 1994). The measurement height was found to be above the urban roughness layer according to the analysis for the flux-gradient relationships of momentum and heat (Moriwaki and Kanda, 2005). The instantaneous horizontal and vertical wind velocities u , v , and w , sonic temperature T , humidity q , and CO₂ concentration c , were sampled at 8 Hz (Table II). To avoid the use of flux corrections arising from density effects (Webb et al.,

TABLE I
Land cover properties at the study site.

Building height	z_H	7.3 m (Std. 1.3 m)
Areal fraction covered by buildings	λ_p	32.6%
Areal fraction covered by vegetation	λ_v	20.6%
Areal fraction of impervious space (paved road + concrete)	λ_I	38.3% (26.2% + 12.1%)
Areal fraction of pervious space (playground except for vegetation)	λ_G	8.5%

Std is the standard deviation.

TABLE II
Instruments and the measured quantities.

Variable	Instrument	Height (m a.g.l.)
u, v, w, Ts	Sonic anemometre (Metek, USA1)	29
c, q	Open path analyzer (Li-Cor, LI-7500)	29

1980), the measured CO_2 mole concentrations were converted into mixing ratios using the sonic temperature. These data were logged to a data logger (CR10X, Campbell Sci.) and stored on a computer.

2.2. DATA PROCESSING

In this study, we used data only from July 2001. To ensure high data quality, we only used data from fair weather days in which the percentage of sunshine exceeded 80%. To determine whether or not a given day was fair, we used weather data from a Japan Meteorological Agency weather station 12.5 km from the tower. In addition, we used only data obtained at local times from 0900 to 1600 during which the meteorological conditions can be regarded as in a quasi steady state; the temporal changes of wind, temperature, humidity, and CO_2 are relatively small at these times. Turbulent statistics were calculated for every 60-min period. There were a total of 43 such periods. The mean meteorological data and fluxes are listed in Table III.

We first eliminated the trend of T , q , and c in each 60-min dataset by subtracting a linear fit to the data and then calculated the following fluctuations from these fits: u' , v' , w' , T' , q' , and c' . Then we transformed the velocity coordinates using a method proposed by McMillen (1988) so that $\overline{v'} = 0$, $\overline{w'} = 0$, and $\overline{v'w'} = 0$.

TABLE III
Conditions measured at the top on the tower (29 m).

Wind speed (m s ⁻¹)	6.8 (2.2)
Wind direction (degree)	187 (22)
Air temperature (°C)	31.0 (1.1)
Water vapor mixing ratio (g kg ⁻¹)	15.5 (0.9)
CO ₂ mixing ratio (mg kg ⁻¹)	563.6 (26.5)
Stability (z/L)	-0.17 (0.1)
Sensible heat flux (W m ⁻²)	283 (69)
Latent heat flux (W m ⁻²)	157 (43)
CO ₂ flux (mg m ⁻² s ⁻¹)	0.24 (0.21)

The values are averages over midday for all fair-weather days in July 2001 and the values in parenthesis are standard deviations.

Following Roth and Oke (1995), we examined the turbulent transfers of heat, water vapour, and CO₂. The analysis was done using the following turbulent linear correlation coefficients:

$$r_{wT} = \overline{w'T'}/\sigma_w\sigma_T = 1/\left(\frac{\sigma_w}{u_*} \frac{\sigma_T}{T_*}\right), \quad (1)$$

$$r_{wq} = \overline{w'q'}/\sigma_w\sigma_q = 1/\left(\frac{\sigma_w}{u_*} \frac{\sigma_q}{q_*}\right), \quad (2)$$

$$r_{wc} = \overline{w'c'}/\sigma_w\sigma_c = 1/\left(\frac{\sigma_w}{u_*} \frac{\sigma_c}{c_*}\right), \quad (3)$$

where the overbar is a time-mean value, the prime denotes the instantaneous deviation from the time-mean value, σ is the standard deviation, and u_* , T_* , q_* , and c_* are the surface-layer scales defined as $(-u'w')^{0.5}$, $\overline{w'T'}/u_*$, $\overline{w'q'}/u_*$, and $\overline{w'c'}/u_*$, respectively. The correlation coefficients can be viewed as a measure of the overall efficiency of the transfer process and varies between 0 (no correlation) and 1 (optimally efficient transfer) (Roth and Oke, 1995).

In addition, we used wavelet analyses to understand the detailed structure of the turbulent transfers. Wavelet analysis provides both scale and time information of analyzed signals and allows an objective separation of patterns in the data that have different time scales at different time. The wavelet technique has recently been applied to micrometeorology (e.g., Gao and Li, 1993; Katul and Vidakovic, 1996; Trevino and Andreas, 1996; Petenko, 2001; Watanabe, 2004), to detect turbulent coherent structures, but it has less been used for the comparison of scalar transfer. One of the

latter studies is Scanlon and Albertson (2001), who applied wavelet analysis to time series of q' and c' within a vegetation canopy and separated respiration from photosynthesis. The wavelet transform of a time series $x(t)$ can be written as

$$W_x(a, b) = \frac{1}{a} \int_0^T f\left(\frac{t-b}{a}\right) x(t) dt, \quad (4)$$

where f represents a wavelet function, a is the dilation parameter, hereafter the time scale, that determines the duration and amplitude of the wavelet, b is the centre of the wavelet, and T is the length of the data record. The wavelet variance is defined as

$$V_x(a) = \int_0^T W_x(a, b)^2 db. \quad (5)$$

We applied wavelet analysis to the time series of w'/σ_w and the turbulent transfers $w'T'/\sigma_w\sigma_T$, $w'q'/\sigma_w\sigma_q$, and $w'c'/\sigma_w\sigma_c$. The transformed time series were normalized by the standard deviations. Therefore, the wavelet coefficients measure the relative intensity of fluctuation to the total turbulent deviation. This enables us to directly compare the efficiency of turbulent transfer of scalars. The analyzing wavelet in this paper is the 'Mexican hat' function, a second derivative of a Gaussian (Figure 2). Because of its functional form, the wavelet transform has large positive values when upward transfers are observed in the original time trace. The choice of analyzing wavelet is not essential for the following result and discussion, as long as we use axisymmetric functions such as 'Morlet', 'Gabor8', and 'Shannon'.

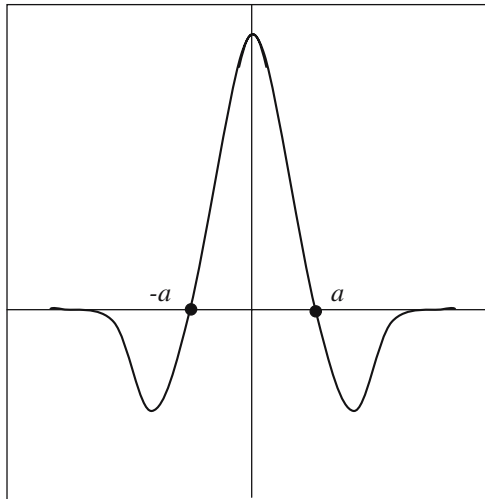


Figure 2. The wavelet function used in the analyses. a is the wavelet time scale.

The turbulent transfers were also inferred using quadrant analysis, a method that is often used for the Reynolds stress fraction in laboratory studies (e.g., Nakagawa and Nezu, 1977; Raupach, 1981; Coppin et al., 1986), large-eddy simulations (e.g., Kanda, 2005), and field experiments (e.g., Shaw et al., 1983; Maitani and Ohtaki, 1987; Bergström and Högström, 1989; Katul et al., 1997b). Quadrant analysis provides the contribution of sweep or ejection motion to the total mean Reynolds stress. In a vegetated canopy, Finnigan (1979) determined that ejection was significant above the canopy but negligible within the canopy. The model simulations of Kanda (2005) found that ejection is dominant in the turbulent flow over urban-like canopies. This ejection dominance also occurs under an unstable urban boundary layer (Oikawa and Meng, 1995).

Quadrant analysis can also be used for the turbulent transfer of scalars. For example, for heat transfer, $w'T'$ is divided into four different quadrants. Quadrants one and three, representing ejection and sweep, respectively, make positive contributions to the vertical heat flux, whereas quadrants two and four make negative contributions to the upward flux. A fraction $S_{i_{wT}}$, which is the conditionally averaged stress $\langle w'T' \rangle_i$ in quadrant i normalized by the total mean averaged heat flux, is defined as

$$S_{i_{wT}} = \langle w'T' \rangle_i / \overline{w'T'}. \quad (6)$$

A similar procedure can be used for water vapour flux $w'q'$ and CO₂ flux $w'c'$ as

$$S_{i_{wq}} = \langle w'q' \rangle_i / \overline{w'q'}, \quad (7)$$

$$S_{i_{wc}} = \langle w'c' \rangle_i / \overline{w'c'}. \quad (8)$$

We used quadrant analysis for the turbulent transfer for heat, water vapour, and CO₂ flux, respectively.

3. Results and Discussion

3.1. CORRELATION COEFFICIENTS BETWEEN w AND SCALARS

First we investigated the ‘global’ similarity of vertical transfer of scalars using the correlation coefficients between w' and T' , w' and q' , and w' and c' , which are defined in Equations (1)–(3) as r_{wT} , r_{wq} , and r_{wc} , respectively. In Figure 3a, 3b, and 3c, they are plotted versus atmospheric stability z'/L , where L is the Obukov length:

$$L = -(\overline{-u'w'})^{3/2} T / gk\overline{w'T'}, \quad (9)$$

where g is the acceleration of gravity, and k is the von Karman constant. Here, $k=0.4$. Momentum transfer efficiency $r_{uw} = -\overline{u'w'}/\sigma_u\sigma_w$ is also plotted by black triangles as reference. The linear correlation coefficient for heat r_{wT} has a positive bias for unstable conditions, compared with the MOS function over flat surfaces (estimated from the combination of Panofsky et al. (1977) and Wyngaard et al. (1971)) indicated by curves in Figure 3. The increased heat transport over that for the flat surfaces is due to the relatively low σ_w/u_* (not shown here). A low σ_w/u_* is commonly observed in urban surface layers (e.g., Clark et al., 1982; Roth and Oke, 1995). The reason for the low σ_w/u_* here is that the relatively high urban roughness increases the momentum transport over that for typical rural areas (Roth and Oke, 1995). The stability dependency of the linear coefficient for water vapour r_{wq} is similar to that of r_{wT} , but it has a smaller magnitude. Also, the linear coefficient for CO₂ mixing ratios r_{wc} is much less than that of r_{wq} . Ohtaki (1985) concluded that temperature and humidity statistics have similar characteristics over fairly homogeneous surfaces. But for more complex surfaces, Beljaars et al. (1983) showed that the nondimensional standard deviations of temperature and humidity have different values at the same stability, as we have found.

Figure 4a and 4b show plots of the ratios of integrated turbulent efficiencies of water vapour to heat r_{wq}/r_{wT} and CO₂ to heat r_{wc}/r_{wT} , respectively. Note that r_{Tq} and r_{Tc} in Figure 4a and 4b, are analogous to the other correlation coefficients in Equations (1)–(3). The data show that the transfer efficiencies of water vapour and CO₂ are smaller than that of heat. The mean value of r_{wq}/r_{wT} and r_{wc}/r_{wT} was 0.55 and 0.22, respectively. The value of r_{wq}/r_{wT} roughly agrees with the urban data of Figure 1c of Roth and Oke (1995), but it is smaller than that estimated from Equations (5) and (6) of Roth and Oke (1995), which are based on the observations from the homogeneous surface layer. According to Katul et al. (1995), the statistics for temperature and humidity could differ because temperature is an active scalar whereas humidity is generally not. Such an argument logically implies then that r_{wT} and others would be relatively alike in near neutral stability but would diverge as $|z'/L|$ increases and temperature assumes a more active role in the dynamics (Andreas et al., 1998). Therefore a stability dependency of r_{wq}/r_{wT} was expected, but it was not found in Figure 4a. The ratio r_{wq}/r_{wT} had a distinct dependency on the correlation coefficient r_{Tq} (see right panel of Figure 4a). Note their r_{Tq} is often used as a measure of the equality of r_{wT} and r_{wq} (De Bruin et al., 1999). Roth and Oke (1995) also show that r_{Tq} is closely related to r_{wq}/r_{wT} . On the other hand, the ratio of CO₂ mixing ratio to heat r_{wc}/r_{wT} decreases as $|z'/L|$ increases. Such a stability dependency is in accordance with the suggestion by Katul et al. (1995). By a similar argument to water vapour, CO₂ might be called 'passive' because the effect of CO₂ on buoyancy is

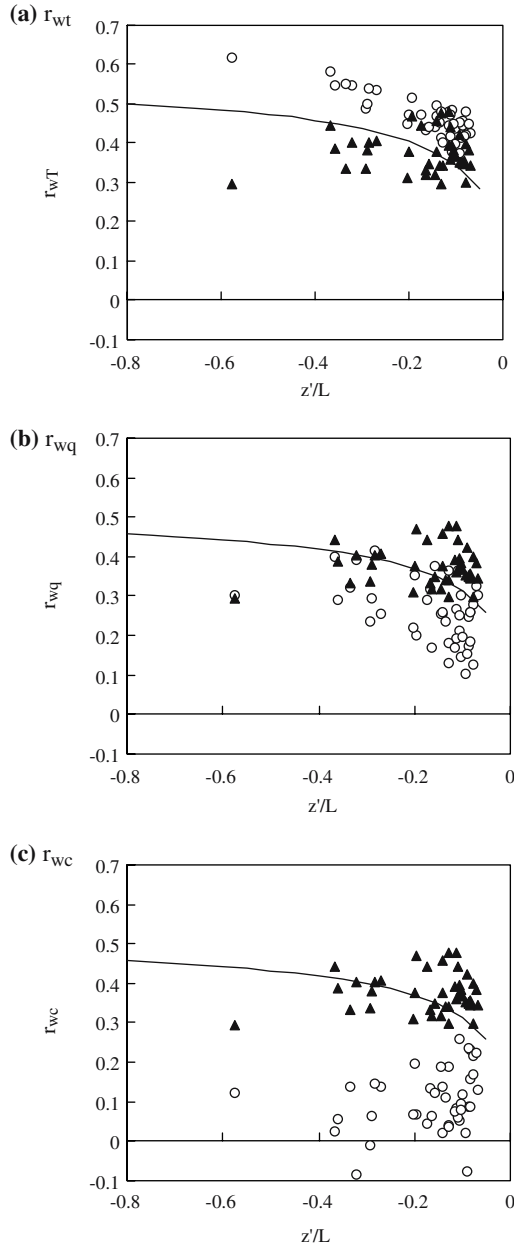


Figure 3. Efficiencies of turbulent transfer for various measured values of atmospheric stability z'/L . Each circle represents one hour of data. (a) Heat transfer efficiency r_{wT} . (b) Water vapour transfer efficiency r_{wq} . (c) CO₂ transfer efficiency r_{wc} . The solid curves are prediction from MOS theory. Momentum transfer efficiency $r_{uw} = -\overline{u'w'}/\sigma_u\sigma_w$ is plotted by black triangle as reference.

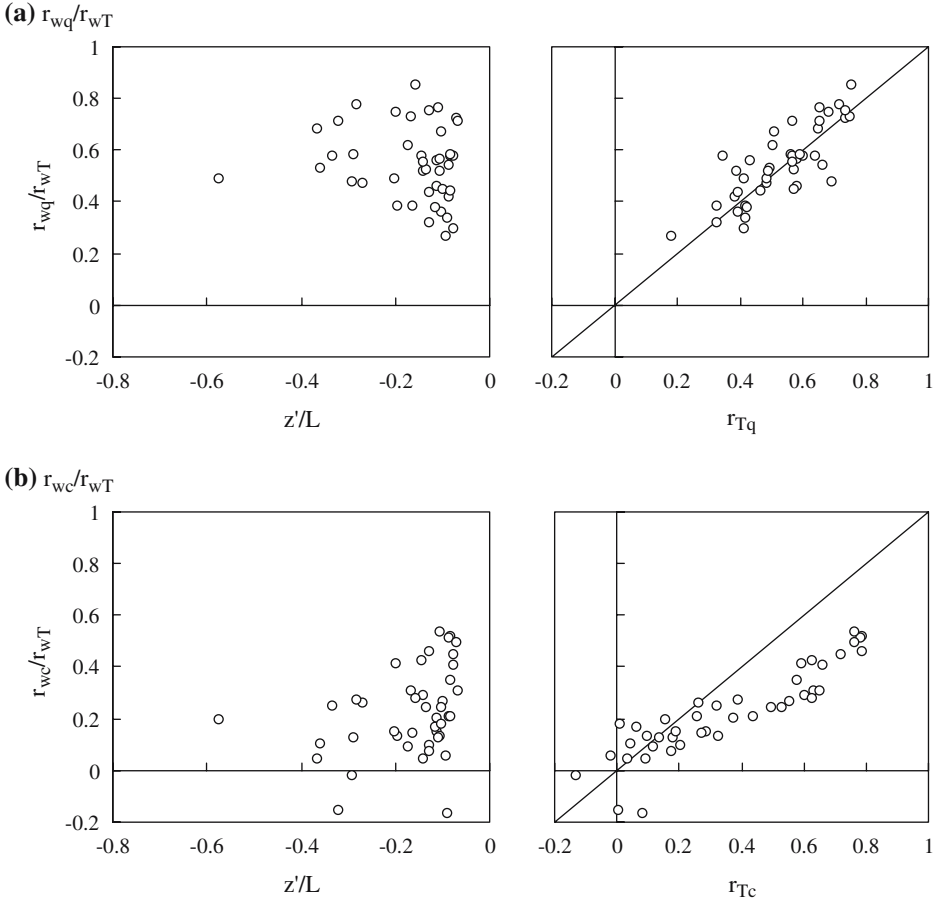


Figure 4. Efficiencies of water vapour and CO₂ turbulent transfer relative to heat transfer versus atmospheric stability (left) and correlation coefficients r_{Tq} and r_{Tc} (right). Each circle represents one hour of data. (a) Water vapour. (b) CO₂.

negligible due to the extremely low mixing ratios of CO₂. The correlation coefficient between temperature and CO₂ concentration r_{Tc} is also a good measure of r_{wc}/r_{wT} , but the proportionality coefficient is about 0.6.

3.2. WAVELET TRANSFORM ON THE TURBULENT TRANSFER OF SCALARS

The wavelet transform is useful for detecting patterns in the data that have different time scales at different times. We investigated the ‘local’ similarity of the turbulent transfer of scalars using the wavelet transform. A typical wavelet transform for the turbulent transfer of scalars is shown in Figure 5. The colour-coding scale at bottom right indicates the value of the wavelet transform. Wavelet analysis was done for the time series data

normalized by the standard deviation of the quantity that was transformed; w'/σ_w , $w'T'/\sigma_w\sigma_T$, $w'q'/\sigma_w\sigma_q$, $w'c'/\sigma_w\sigma_c$, T'/σ_T , q'/σ_q , and c'/σ_c . Hence, the value shows the intensity of turbulent transfer relative to the total flux of scalars (see Section 2.2). We now compare the turbulent transfers of scalars.

First, we point out the common features between the scalar transfers. Small time-scale turbulence (i.e., $a < 1$ s) has no specific organized structures for the vertical velocity w'/σ_w as shown in the upper most region of Figure 5a (between 1 and 0.25 s). The same applies to the turbulent transfer of $w'T'/\sigma_w\sigma_T$, $w'q'/\sigma_w\sigma_q$, and $w'c'/\sigma_w\sigma_c$ (Figures 5b–5d). This disorganized small-scale turbulence field is contributed primarily by random background turbulence at small scales. As the time scale increases, the distribution tends to be organized into discrete structures. These organized structures can be divided into two time scales. Figure 6 shows the resulting scalogram for the wavelet variance of $w'T'/\sigma_w\sigma_T$, $w'q'/\sigma_w\sigma_q$, and $w'c'/\sigma_w\sigma_c$ obtained from Figure 5. The scalogram has a plateau near $a = 8$ s

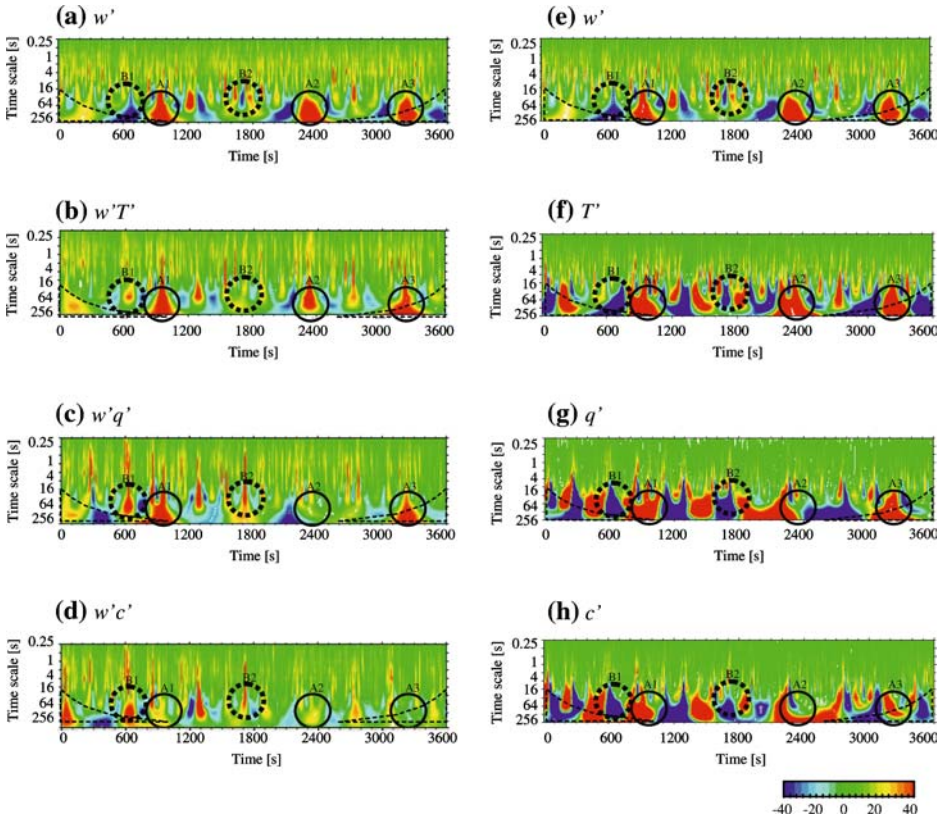


Figure 5. Wavelet transforms using various time scales a for variables measured from 1300 to 1400 on 11 July 2001. (a) w'/σ_w , (b) $w'T'/\sigma_w\sigma_T$, (c) $w'q'/\sigma_w\sigma_q$, (d) $w'c'/\sigma_w\sigma_c$, (e) w'/σ_w , (f) T'/σ_T , (g) q'/σ_q , and (h) c'/σ_c . Circles mark thermal structures.

and a peak near $a = 64$ s. For the ‘Mexican hat’ wavelet function, as we use here, a can be roughly converted to the spectral frequency $f = (4a)^{-1}$; thus these time scales correspond to 32 and 256 s of the period of the sine wave. The structures with a time scale of 32 s are probably surface layer eddies, because the nondimensional frequency $n_m (= 0.09)$ of these structures is consistent with the surface layer relationship developed from field experiments (Kaimal and Finnigan, 1994). Another structure group can be found in the time scales from 256 s. In these structures, heat is positively transferred from the surface to the atmosphere. These structures correspond to the updraft motions that occurred at the same time and with the same time scale in Figure 5a. The long time scale of these structures (256 s) suggests that these structures are thermals or rolls (e.g., Stull, 1988).

Second, we discuss the dissimilarity of turbulent transfers of scalars. In the structures marked by circles (A1–A3) in Figure 5, heat is always transferred upward by structures with positive vertical velocity. However, for some of these structures, water vapour and CO₂ are either not transferred or are only weakly transferred (see Figures 5c and 5d). Possible reasons for the dissimilarity for the transfer efficiency among scalars are the physical characteristics and the heterogeneity in the source distribution of scalars. Heat is an active scalar and produces the thermal structures by itself. Hence, the heat is most efficiently transferred. On the other hand, water vapour and CO₂ have less contribution to the buoyant convection. If their horizontal distributions were homogeneous near the surface (as they are for crops and forests), they would be transferred as well as heat. However, in the urban surface there are complex source and sink patterns of scalars (e.g., Roth and Oke, 1995). Moriwaki and Kanda (2004) showed that the main source of H₂O is from vegetation and that of CO₂ is from houses, transportation, and human exhalations. The heterogeneity of sinks and sources would produce a similar heterogeneity in the concentration in

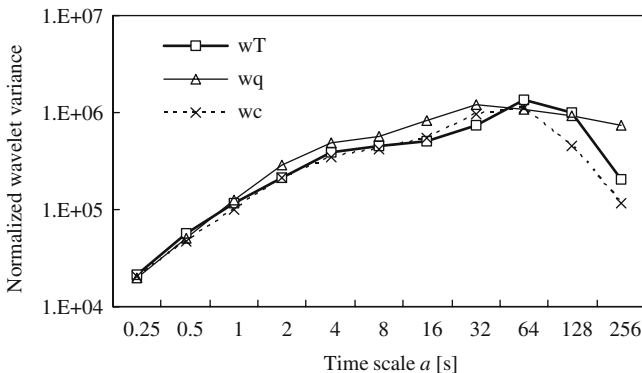


Figure 6. Wavelet variance for $w'T'/\sigma_w\sigma_T$, $w'q'/\sigma_w\sigma_q$, and $w'c'/\sigma_w\sigma_c$ from data in Figure 5.

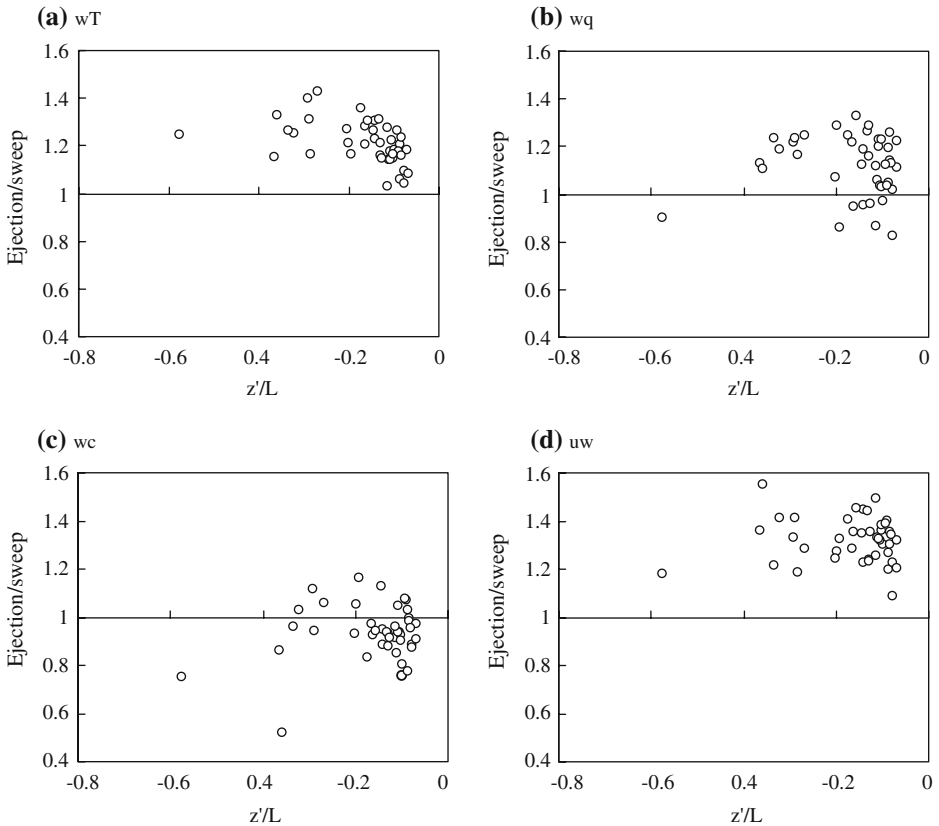


Figure 7. Fractional ratio of ejection to sweep for turbulent transfer of (a) heat, (b) water vapour, (c) CO₂, and (d) momentum. Each circle represents one hour of data.

the urban boundary layer. As a result, the heterogeneity increases the variance of that variable but not necessarily its flux (Weaver, 1990). Under such a condition, some thermal structures may also transfer the scalars but other thermal structures would not because the position of a thermal might have little correlation with the region or high humidity of CO₂ mixing ratio.

We also analyzed the downward motions. The structures marked by dotted circles (B1–B2) in Figure 5 are downward motions. In these structures, water vapour and CO₂ were efficiently transferred upward, whereas heat was not transferred. We analyze these structures further in the next section.

3.3. RELATIVE CONTRIBUTION OF EJECTION AND SWEEP

A dissimilarity in turbulent transfers was also found using quadrant analyses. The quadrant analyses determine the contributions of sweep or ejection

motions to the total fluxes in terms of a 'global' index. Figure 7 shows the relative contributions to flux by ejection and sweep for heat, water vapour, CO₂, and momentum transfer for various values of atmospheric stability. The ejection/sweep ratio for heat is larger than unity when z/L is most negative. This is similar to the results for the atmospheric surface layer over natural ecosystems such as rice paddies, bare soil, water surfaces, and deciduous forests (Maitani and Ohtaki, 1987; Maitani and Shaw, 1990). The ejection dominance in unstable conditions is associated with thermally generated turbulence. In contrast, the ejection/sweep ratio of water vapour transfer is less than that of heat transfer. Mahrt (1991) and De Bruin et al. (1993) pointed out that when the surface evaporation is lower, the statistics of water vapour are affected by downward motions related to the entrainment of warm dry air from aloft. Wavelet analysis in the previous section also shows that upward water vapour transfer occurs in downward motions (dotted circles in Figure 5). The ejection/sweep ratio of CO₂ transfer is even less than that of water vapour. This indicates that downward motion (sweep) transfers CO₂ more efficiently than ejections. CO₂ near the ground has a strong inhomogeneity in its spatial distribution. Therefore, CO₂ is not always transferred by thermals as well as heat or water vapour. On the other hand, the heterogeneity of scalars in the upper air is generally less than that near the surface according to concepts of blending height (e.g., Mahrt, 2000). Therefore, in downward motions, the lower CO₂ is efficiently transferred.

4. Concluding Remarks

The 'local' and 'global' similarity of vertical turbulent transfer of heat, water vapour, and CO₂ were examined in an urban surface layer over a residential area in Tokyo, Japan. We investigated the correlation coefficients and examined the quadrant analysis for the 'global' similarity and we also examined the wavelet analysis for the 'local' similarity. The ratios of linear correlation coefficients for water vapour/heat and CO₂/heat showed that the transfer efficiencies of water vapour and CO₂ were smaller than that of heat in unstable conditions, a result that conflicts with conventional surface-layer theory. The wavelet analysis showed that heat was always transferred efficiently by the thermal structures and organized structures. Water vapour and CO₂ were transferred as well as heat in some of the structures, but not in others. The quadrant analyses also indicated that water vapour and CO₂ were transferred less by upward turbulent motions compared with the heat transport. These differences between heat and both CO₂ and water vapour were probably caused both by the active role of temperature and the heterogeneity in the source distribution of scalars. Heat is an active

scalar and produces the thermal structures. Hence, the heat is transferred most efficiently. Water vapour and CO₂ are transferred passively. If their horizontal distributions were homogeneous, they would be transferred as well as heat. However, the sinks/sources of water vapour and CO₂ are inhomogeneous. As a result, the heterogeneities of water vapour and CO₂ concentrations decrease their transfer efficiencies.

Acknowledgements

This study was financially supported by CREST (Core Research for Evolution Science and Technology) of JST (Japan science and Technology Agency) and by a Grant-in-Aid for Developmental Scientific Research from the Ministry of Education, Science and Culture of Japan. We thank Rev. Sister R. Kugimiya who kindly offered the land space for the field measurements.

References

- Andreas, E. L., Hill, R. J., Gosz, J. R., Moore, D. I., Otto, W. D., and Sarma, A. D.: 1998, 'Statistics of Surface Layer Turbulence over Terrain with Meter-Scale Heterogeneity', *Boundary-Layer Meteorol.* **86**, 379–408.
- Asanuma, J. and Brutsaert, W.: 1999, 'The Effect of Chessboard Variability of the Surface Fluxes on the Turbulence Fields in a Convective Atmospheric Surface Layer', *Boundary-Layer Meteorol.* **91**, 37–50.
- Baldocchi, D. and Wilson, K.: 2001, 'Modeling CO₂ and Water Vapor Exchange of a Temperate Broadleaved Forest across Hourly to Decadal Time Scales', *Ecol. Model.* **142**, 155–184.
- Beljaars, A. C. M., Schotanus, P., and Nieuwstadt, F. T. M.: 1983, 'Surface Layer Similarity under Nonuniform Fetch Conditions', *J. Clim. Appl. Meteorol.* **22**, 1800–1810.
- Bergström, H. and Högström, U.: 1989, 'Turbulent Exchange Above a Pine Forest II: Organized Structures', *Boundary-Layer Meteorol.* **49**, 231–263.
- Clark, J. F., Ching, J. K. S., and Godowitch, J. M.: 1982, An Experimental Study of Turbulence in an Urban Environment, Tech. Report EPA-600/3-82-062, U. S. EPA, Research Triangle Park, NC, p. 150.
- Coppin, P. A., Raupach, M. R., and Legg, B. J.: 1986, 'Experiments on Scalar Dispersion within a Model Plant Canopy Part II: An Elevated Plane Source', *Boundary-Layer Meteorol.* **35**, 167–191.
- De Bruin, H. A. R., Kohsiek, W., and Van den Hurk, B. J. J. M.: 1993, 'A Verification of Some Methods to Determine the Fluxes of Momentum, Sensible Heat, and Water Vapor, Using Standard Deviation and Structure Parameter of Scalar Meteorological Quantities', *Boundary-Layer Meteorol.* **63**, 231–257.
- De Bruin, H. A. R., Van Den Hurk, B. J. J. M., and Kroon, L. J. M.: 1999, 'On the Temperature-Humidity Correlation and Similarity', *Boundary-Layer Meteorol.* **93**, 453–468.
- Finnigan, J. J.: 1979, 'Turbulence in Waving Wheat. I. Mean Statistics and Honami', *Boundary-Layer Meteorol.* **16**, 181–211.

- Gao, W. and Li, B. L.: 1993, 'Wavelet Analysis of Coherent Structures at the Atmosphere-forest Interface', *J. Appl. Meteorol.* **32**, 1717–1725.
- Grimmond, C. S. B., King, T. S., Cropley, F. D., Nowak, D. J., and Souch, C.: 2002, 'Local-scale Fluxes of Carbon dioxide in Urban Environments: Methodological Challenges and Results from Chicago', *Environ. Poll.* **116**, S243–S254.
- Kaimal, J. C. and Finnigan, J. J.: 1994, *Atmospheric Boundary Layer Flows: Their Structure and Measurement*, Oxford University Press, New York, NY, p. 289.
- Kanda, M.: 2005, 'Large Eddy Simulations on the Effects of Surface Geometry of Building Arrays on Turbulent Organized Structures', *Boundary-Layer Meteorol.* In press.
- Katul, G., Goltz, S. M., Hsieh, C.-I., Cheng, Y., Mowry, F., and Sigmon, J.: 1995, 'Estimation of Surface Heat and Momentum Fluxes Using the Flux-Variance Method above Uniform and No-Uniform Terrain', *Boundary-Layer Meteorol.* **74**, 237–260.
- Katul, G. and Vidakovic, B.: 1996, 'The Partitioning of Attached and Detached Eddy Motion in the Atmospheric Surface Layer Using Lorentz Wavelet Filtering', *Boundary-Layer Meteorol.* **77**, 153–172.
- Katul, G., Kuhn, G., Schiedge J., and Hsieh, C.-I.: 1997a, 'The Ejection-Sweep Character of Scalar Fluxes in the Unstable Surface Layer', *Boundary-Layer Meteorol.* **83**, 1–26.
- Katul, G., Hsieh, C.-I., Kuhn, G., and Ellsworth, D.: 1997b, 'Turbulent Eddy Motion at Forest-atmosphere Interface', *J. Geophys. Res.* **102**, 13409–13421.
- Katul, G. and Hsieh, C.-I.: 1999, 'A Note on the Flux-variance Similarity Relationships for Heat and Water Vapour in the Unstable Atmospheric Surface Layer', *Boundary-Layer Meteorol.* **90**, 327–338.
- Mahrt, L.: 1991, 'Boundary-Layer Moisture Regimes', *Quart. J. Roy. Meteorol. Soc.* **117**, 151–176.
- Mahrt, L.: 2000, 'Surface Heterogeneity and Vertical Structure of the Boundary Layer', *Boundary-Layer Meteorol.* **96**, 33–62.
- Maitani, T. and Ohtaki, E.: 1987, 'Turbulent Transport Processes of Momentum and Sensible Heat in the Surface Layer over a Paddy Field', *Boundary-Layer Meteorol.* **40**, 283–293.
- Maitani, T. and Shaw, R. H.: 1990, 'Joint Probability Analysis of Momentum and Heat Fluxes at a Deciduous Forest', *Boundary-Layer Meteorol.* **52**, 283–300.
- McMillen, R. T.: 1988, 'An Eddy Correlation Technique with Extended Applicability to Non-simple Terrain', *Boundary-Layer Meteorol.* **43**, 231–245.
- Moriwaki, R. and Kanda, M.: 2004, 'Seasonal and Diurnal Fluxes of Radiation, Heat, Water Vapor and CO₂ over a Suburban Area', *J. Appl. Meteorol.* **43**, 1700–1710.
- Moriwaki, R. and Kanda, M.: 2005, 'Flux-gradient Profiles for Momentum and Heat over an Urban Surface', *Theor. Appl. Climatol.* doi:10.1007/s00704-005-0150-3.
- Nakagawa, H. and Nezu, I.: 1977, 'Prediction of the Contributions to the Reynolds Stress from Bursting Events in Open-channel Flow', *J. Fluid Mech.* **80**, 99–128.
- Ohtaki, E.: 1985, 'On the Similarity in Atmospheric Fluctuation of Carbon dioxide, Water vapor and Temperature over Vegetated Fields', *Boundary-Layer Meteorol.* **32**, 25–37.
- Oikawa, S. and Meng, Y.: 1995, 'Turbulence Characteristics and Organized Motion in a Suburban Roughness Sublayer', *Boundary-Layer Meteorol.* **74**, 289–312.
- Panofsky, H. A., Tennekes, H., Lenschow, D. H., and Wyngaard, J. C.: 1977, 'The Characteristics of Turbulent Velocity Components in the Surface Layer under Unstable Conditions', *Boundary-Layer Meteorol.* **11**, 355–361.
- Petenko, I. V.: 2001, 'Advanced Combination of Spectral and Wavelet Analysis ("Spavelet" Analysis)', *Boundary-Layer Meteorol.* **100**, 287–299.
- Raupach, M. R.: 1981, 'Conditional Statistics of Reynolds Stress in Rough-wall and Smooth-wall Turbulent Boundary Layers', *J. Fluid Mech.* **108**, 363–382.

- Roth, M. and Oke, T. R.: 1995, 'Relative Efficiencies of Turbulent Transfer of Heat, Mass, and Momentum over a Patchy Urban Surface', *J. Atmos. Sci.* **52**, 1863–1874.
- Scanlon, T. M. and Albertson, J. D.: 2001, 'Turbulent Transport of Carbon dioxide and Water vapor within a Vegetation Canopy during Unstable Conditions: Identification of Episodes Using Wavelet Analysis', *J. Geophys. Res.* **106(D7)**, 7251–7262.
- Sempreviva, A. M. and Høstrup, J.: 1998, 'Transport of Temperature and Humidity Variance and Covariance in Coastal Atmospheric Boundary Layers', *Boundary-Layer Meteorol.* **87**, 233–253.
- Shaw, R. H., Tavangar, J., and Ward, D.: 1983, 'Structure of the Reynolds Stress in a Canopy Layer', *J. Clim. Appl. Meteorol.* **22**, 1922–1931.
- Stull, R. B.: 1988, *An Introduction to Boundary Layer Meteorology*, Kluwer Academic Publishers, The Netherlands, 666 pp.
- Tillman, J. E.: 1972, 'The Indirect Determination of Stability, Heat and Momentum Fluxes in the Atmospheric Boundary Layer from Simple Scalar Variables during Dry Unstable Conditions', *J. Appl. Meteorol.* **11**, 783–792.
- Trevino, G. and Andreas, E.: 1996, 'On Wavelet Analysis of Nonstationary Turbulence', *Boundary-Layer Meteorol.* **81**, 271–288.
- Watanabe, T.: 2004, 'Large-eddy Simulation of Coherent Turbulence Structures Associated with Scalar Ramps over Plant Canopies', *Boundary-Layer Meteorol.* **112**, 307–341.
- Weaver, H. J.: 1990, 'Temperature and Humidity Flux-variance Relations Determined by One-Dimensional Eddy Correlation', *Boundary-Layer Meteorol.* **53**, 77–91.
- Webb, E. K., Pearman, G. I., and Leuning, R.: 1980, 'Correction of Flux Measurements for Density Effects Due to Heat and Water vapour Transfer', *Quart. J. Roy. Meteorol. Soc.* **106**, 85–100.
- Wesely, M. L.: 1988, 'Use of Variance Techniques to Measure Dry Air-Surface Exchange Rates', *Boundary-Layer Meteorol.* **44**, 13–31.
- Wyngaard, J. C., Coté, O. R., and Izumi, Y.: 1971: 'Local Free Convection, Similarity and the Budgets of Shear Stress and Heat Flux', *J. Atmos. Sci.* **37**, 271–284.